GENERAL ATOMIC

DIVISION OF

GENERAL DYNAMICS

JOHN JAY HOPKINS LABORATORY FOR PURE AND APPLIED SCIENCE

P.O. BOX 608, SAN DIEGO, CALIFORNIA 92112

GACD-6249
(2/28/65)
5

RADIATION EFFECTS ON SILICON

Third Quarterly Progress Report Covering the Period
December 1, 1964, through February 28, 1965

Work done by:

L. A. Berry
S. K. Boehm
R. E. Dutton
H. Horiye
A. Kozoman
D. K. Nichols
D. P. Snowden
V. A. J. van Lint
M. E. Wyatt

Report written by:

D. K. Nichols
D. P. Snowden
V. A. J. van Lint

National Aeronautics and Space Administration
Contract NAS7-289
Project 430

March 15, 1965

I. INTRODUCTION

This third quarterly report on Contract NAS7-289, Radiation Effects in Silicon Solar Cells," covers the period December 1, 1964, through February 28, 1965. This report will discuss accomplishments in two specific areas: (1) measurements by electron-spin resonance of the silicon G-8 and the vacancy-phosphorus defects, and (2) measurement of the excess-carrier dependence of the lifetime in p-type silicon to determine the active recombination center.

II. ESR MEASUREMENTS

2.1 INTRODUCTION

During this quarter measurements of the introduction rate of the silicon G-8 center, the vacancy-phosphorus defect, have been completed. Preliminary results from these measurements were given in the last quarterly report.[1]

Measurements of the silicon G-6 center (formerly called the J-center), the divacancy in p-type material, have been performed on floating-zone material irradiated with 6, 15 and 30 MeV electrons at 300°K.

2.2 RESULTS AND CONCLUSIONS

2.2.1 The Vacancy-Phosphorus Center

Angular dependent studies of the resonance signals of the G-8 center samples discussed in Reference 1 have been completed providing more reliable data on the energy-dependent production rate for this center. The introduction rates obtained at the three irradiation energies studied are shown in Table 1 and plotted in Fig. 1.

Table 1

INTRODUCTION RATES OF VACANCY-PHOSPHORUS COMPLEX IN SILICON IRRADIATED AT 300°K

Irradiation Energy (MeV)	Introduction Rate (cm^{-1})
8	0.032
15	0.041
30	0.059

level is between E_V and $E_V + 0.25$ eV. On irradiation, the concentration of the G-6 center, the divacancy, therefore increases linearly with flux until the acceptor levels are depopulated.

The measurements reported here were performed on floating-zone silicon doped with 1.2×10^{17} cm^{-3} boron. Irradiations were performed at $300^{o}K$ with 6, 15 and 30 MeV electrons. Resonance measurements were performed at $4.2^{o}K$ since the more lightly irradiated sample carriers are thermally excited from the acceptor levels at higher temperatures, causing an increased sample conductivity and therefore a reduced cavity Q. This in turn would reduce the sensitivity of the apparatus. The divacancy resonance signals are large and easily measured. In addition, complications due to the presence of other resonance signals are absent which aids in an accurate determination of signal magnitudes. In Table 2 are shown the number of samples irradiated at each energy, the range of fluxes used and the introduction rates obtained. These results are also plotted in Fig. 1.

Table 2

INTRODUCTION RATES OF DIVACANCIES OF FLOATING ZONE p-TYPE SILICON IRRADIATED AT $300^{o}K$

Irradiation Energy (MeV)	Number of Samples Irradiated	Range of Fluxes (cm^{-2})	Introduction Rate (cm^{-1})
6	3	5.7 to 23×10^{16}	0.055
15	4	4.7 to 19.5×10^{16}	0.063
30	4	4.8 to 50×10^{16}	0.095

It should be pointed out that the introduction rates obtained here are for the total production of divacancies, both those formed directly by the incident electrons <u>and</u> those subsequently formed by the combination of single vacancies. As has been pointed out by Watkins and Corbett[2] these two contributions to the divacancy production rate may be separated by studying the introduction rate of divacancies in pulled material. The large quantity of oxygen contained in this material acts as an efficient trap for single vacancies and prevents their combination to form divacancies. We have not yet measured the introduction rate in pulled material.

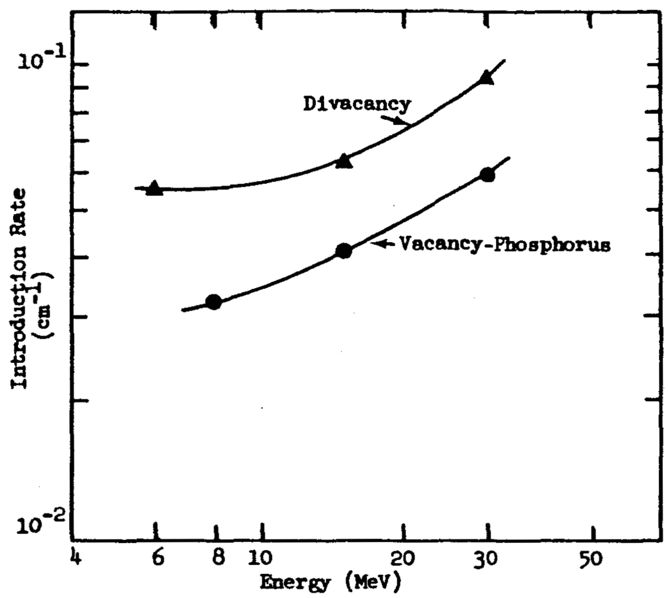

Fig. 1--Energy dependence of the introduction rates of divacancies in floating-zone grown p-type silicon and the vacancy-phosphorus complex in floating-zone grown n-type silicon. Irradiations were performed at 300°K.

As is always the case for absolute intensity measurements of microwave resonance signals, the absolute accuracy of these results is very difficult to assess, and errors could be as high as plus or minus a factor of two. The relative accuracy of the results is, however, much better than this, and from the fluctuation of the data at different fluxes for each energy we estimate this accuracy to be ± 15%. The introduction rates quoted in Table 1 are determined from the G-8 center concentration and the flux needed to obtain that concentration and therefore are the introduction rates for the vacancy-phosphorus complex, assuming linear production beginning at zero flux. An accurate determination of the rate of appearance of the G-8 center has not been possible since the absolute sensitivity of the spin-resonance apparatus does not permit measurement of G-8 center concentration at sufficiently low concentrations to accurately determine the threshold flux at which the center first appears as the Fermi level approaches E_c - 0.4 eV.

2.2.2 The Divacancy in Floating-Zone p-Type Silicon

The divacancy has recently been discussed in considerable detail by Watkins and Corbett.[2] The divacancy in p-type material is seen in spin resonance when the level is singly positively charged, when the Fermi

Previously we have discussed a small discrepancy between our measured g-values for the G-8 center and those reported by Watkins and Corbett, our values being 0.0005 below theirs. It should be mentioned that we also observe a difference for the G-6 center, our values being 0.0003 below theirs. Since these differences are both within the stated experimental error, no great significance should be inferred from this observation, except that evidently a small systematic difference in the determination of the g-values does exist between the two laboratories.

2.3 FUTURE WORK

Measurements of the introduction rate of directly formed divacancies will be performed for direct comparison with the tentative high-energy results of Watkins and Corbett.[2] These measurements await the arrival of the supplier of pulled p-type silicon material.

Samples are now being prepared for studies of the introduction rates of G-6 and G-8 centers irradiated in the 1 to 3 MeV range. These irradiations will be performed using the General Dynamics/Convair Dynamitron facility.

III. LIFETIME MEASUREMENTS

3.1 INTRODUCTION

During the previous quarter lifetime measurements were performed on n- and p-type silicon, both by the dc conductivity technique and the microwave conductivity technique. Inadequate control over the sample temperature limited the accuracy of the microwave measurements, and some further emphasis has been placed on the dc conductivity measurements. Meanwhile, under another program the microwave method had been improved and is being subjected to further calibration checks prior to utilization in determining the injection level dependence of the lifetime. The dc conductivity experiments have also been developed further and analysis has been performed of some experiments with p-type samples.

It has previously been pointed out that the assumption of individual carrier lifetimes, τ_{no} and τ_{po}, which are independent of temperature, are inconsistent with the experimental data. Hence a summary of the literature has been compiled to evaluate the current status of knowledge on temperature dependence of the recombination cross section.

3.2 EXPERIMENTAL TECHNIQUES

The primary difficulty with measurements by the dc conductivity technique on p-type silicon at low temperature has been contact rectification. This problem is manifested by a relative change in contact resistance which is much larger than the change in sample resistivity. In this way the change in conductivity must be calculated as a small difference between a large change in current and voltage simultaneously. This problem is illustrated by the formula for the change in conductivity,

$$\frac{\Delta\sigma}{\sigma_o} = \frac{\frac{\Delta I}{I_o} - \frac{\Delta V}{V_o}}{1 + \frac{\Delta V}{V_o}} .$$

If there is no significant contact rectification problem, $\frac{\Delta I}{I_o}$ is positive and $\frac{\Delta V}{V_o}$ is negative, and the terms in the numerator are accumulative. However, at low temperatures we observe $\frac{\Delta V}{V_o}$ to be positive and almost the same size as $\frac{\Delta I}{I_o}$.

Another problem which has been encountered in making measurements of the extremely short lifetimes that are frequently prevalent at low temperatures is that the capacitance in the measuring circuit, together with the contact resistance, represents a circuit relaxation time which masks a short lifetime. This effect is illustrated in Fig. 2. The sample hookup and the equivalent circuit, including stray capacitance, are also shown in Fig. 2. The resistances, R_{CI1} and R_{CI2} represent the contact impedances at the current contacts. The capacitances C_{S1} and C_{S2} represent the effective capacitance of the sample to ground. The resistances R_{CV1} and R_{CV2} are the contact impedances of the voltage probes, and the capacitances C_{V1} and C_{V2} are the capacitances to ground of the measuring circuit connected to the voltage probes.

Experiments have been performed which illustrate that all four capacitances shown in the diagram have a severe effect on the measuring circuit. Specifically, when a sharp current pulse was applied from the pulser, the voltage pulse was observed to overshoot and the current pulse undershot. This observation indicates that the capacitances C_{S1} and C_{S2} allowed the current to bypass the 100 ohm measuring resistor until a time $\sim R_{CI2}$ times the effective parallel capacitances in the sample and measuring circuit. It was also observed that decreasing the capacitances on the voltage measuring circuits, C_{V1} and C_{V2}, appreciably sharpened up the measured current pulse. The 100 ohm measuring resistance multiplied by any reasonable circuit capacitance could not account for this behavior, and hence it must be determined by the contact resistance. This observation was made even at room temperature and the phenomenon becomes even more severe at low temperatures.

As a result of this observation, an improvement was made in the measuring circuit. In order to minimize the capacitances C_{V1} and C_{V2}, a pair of identical cathode-follower circuits were mounted next to the semiconductor sample to minimize the amount of interconnecting circuit capacitance. Recent experiments have been performed with this improved configuration, and the results of these experiments are now being analyzed. At first sight, the problems with circuit capacitance and contact rectification have not been solved completely, but the measurements appear to be more reliable than earlier ones.

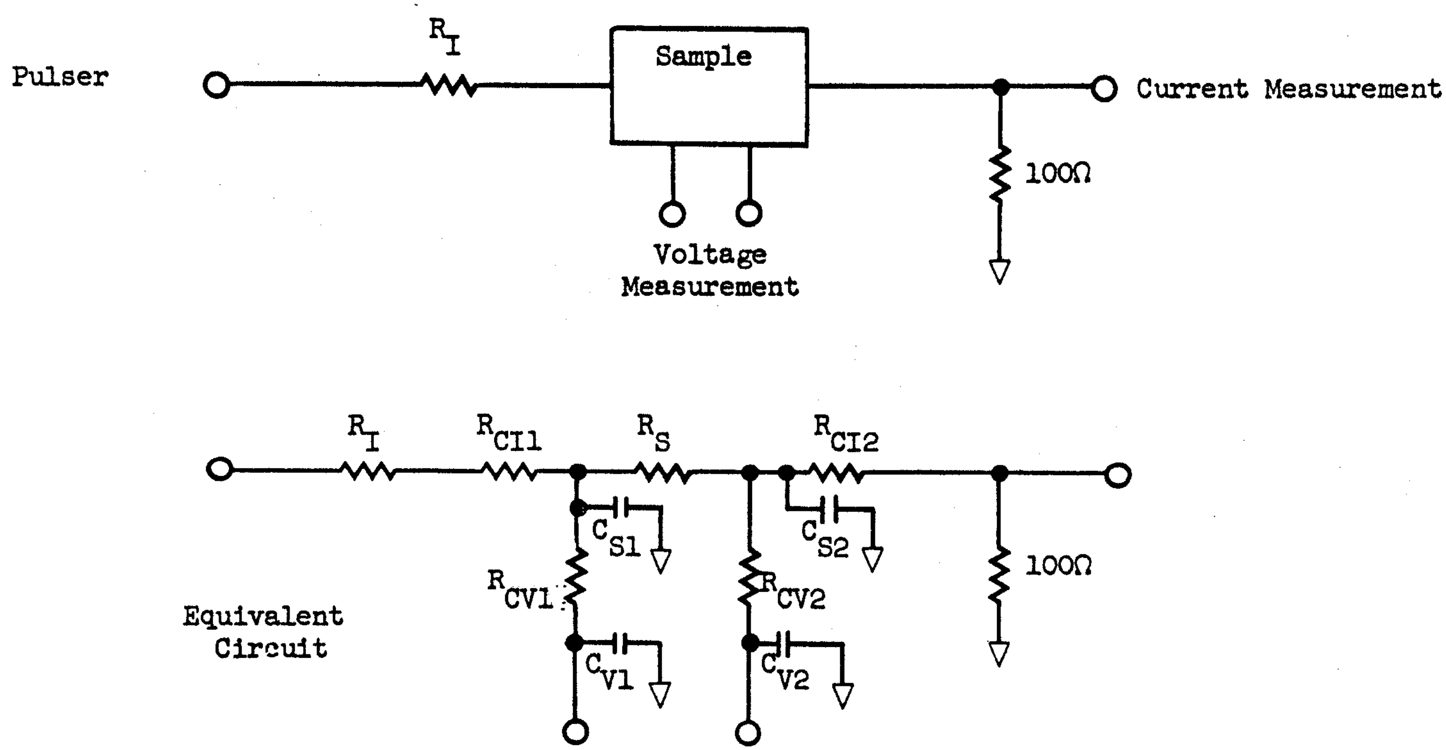

Fig. 2--Capacitance effects in measuring circuit

3.3 TEMPERATURE DEPENDENCE OF RECOMBINATION CROSS SECTIONS IN SILICON

The temperature dependence of attractive and neutron recombination centers in silicon has been calculated from the theory of Lax.[3] Lax's "giant trap" theory assumes that an electron is captured into an excited state of large radius for which it has a certain "sticking probability" of reaching the lowest stable bound state by a cascade of low-energy transitions. The energy lost by the electron is given off by one-phonon processes which may be of either the acoustic or optical mode. It turns out that the acoustic processes dominate at temperatures near absolute zero and the optical processes are most important in the $70^{o}K$ to $400^{o}K$ temperature range considered here.

Lax's calculation for the attractive cross section for the latter processes gives:

$$\sigma_{(opt)}(T) = \sigma_o \lambda \left[1 - \exp(-\lambda)\right]^{-1} D(\lambda) \qquad (1)$$

where

$$\sigma_o = \frac{8\pi}{15}\left(\frac{E_2}{E_1}\right)^2 \frac{Z^3}{\ell} \frac{e^2}{KkT}\left(\frac{e^2}{K\hbar\omega}\right)^2 \qquad (2)$$

is a unit of cross section independent of temperature, $\lambda = \hbar\omega/kT$, and $D(\lambda)$ is a special function which is tabulated. For silicon the energy for the optical phonons is $\hbar\omega = 0.06$ eV, the ratio of the squares of the deformation constants for the two modes $(E_2/E_1)^2 \approx 1$, the mean free path at room temperature is $\ell = 320$ Å, the dielectric constant $K = 16$, and the other constants have their usual meaning. Thus, for a singly charged center ($Z = 1$), $\sigma_o = 10^{-14}$ cm^2. The temperature dependence given by Eq. (1) is plotted in Fig. 3.

The magnitude of the calculated cross section is larger than those determined from experiment. Two possible reasons for the overestimate are:

1) The sticking probability has been estimated from the value calculated for emission and absorption of acoustic phonons only, whereas qualitative considerations show that the probability of escape for the electron is greater for optical phonon transitions.

2) The strictly classical calculation used to derive Eq. (1) will be somewhat of an overestimate since it includes some transitions to binding energies larger than the ground-state binding energy.

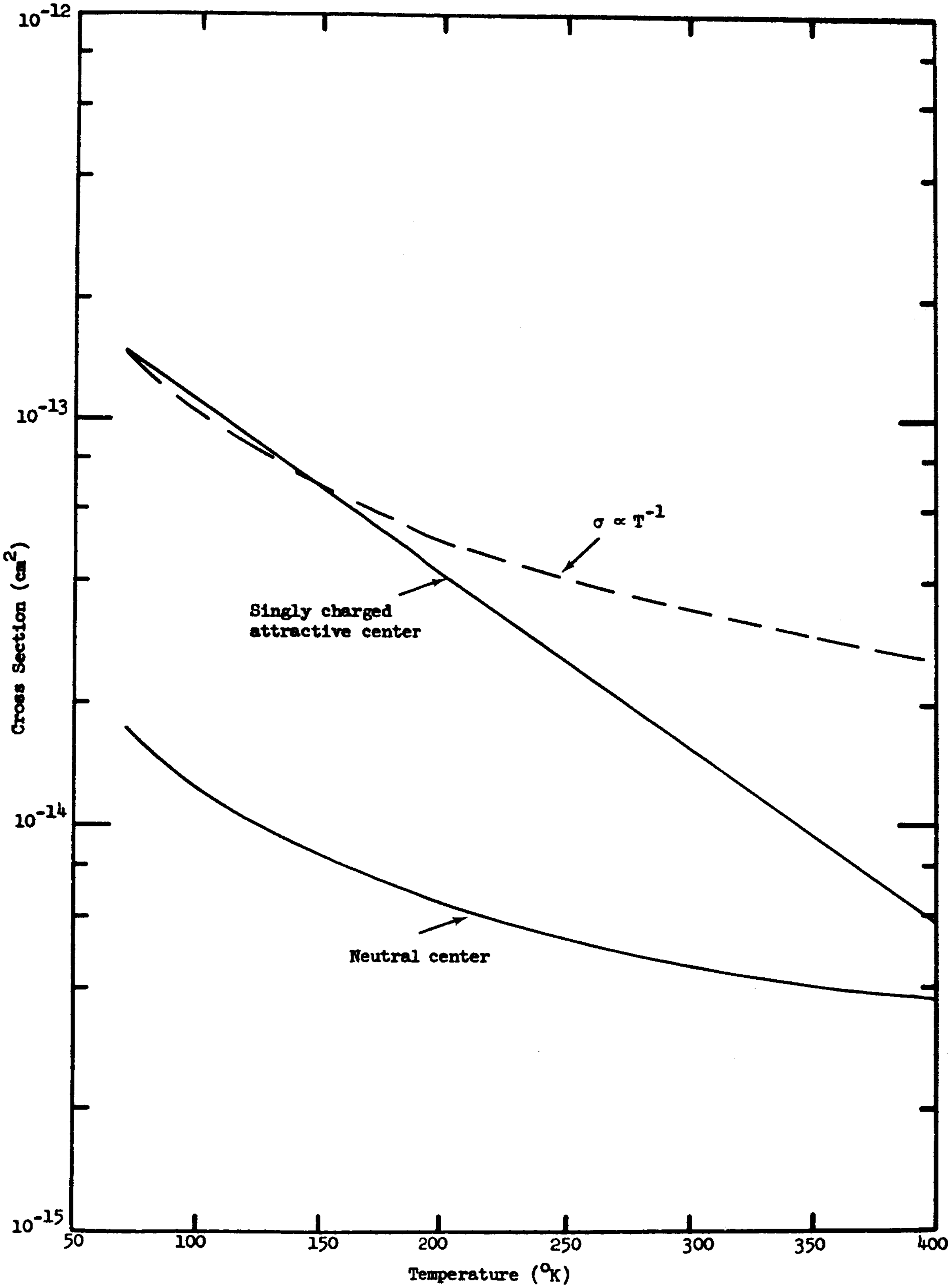

Fig. 3--Recombination cross section of silicon vs. temperature

The calculation for electron capture by a neutral center has also been given. Lax assumes a polarization potential of the form $V \propto 1/r^4$ for which no stationary closed orbits exist. The electron will spiral inward and it is assumed that the sticking probability is essentially unity. The formula for the neutral cross section is:

$$\sigma = 1.7 \times 10^{-15} \lambda \left[1 - \exp(-\lambda)\right]^{-1} \text{cm}^2 \qquad (3)$$

whose temperature dependence is nearly 1/T for the temperature range of interest. This cross section, which is also larger than experimental values, is given in Fig. 3.

The major assumptions which have gone into the above calculations are the use of classical mechanics and a sticking probability depending only on binding energy. Other simplifying assumptions, which may affect the magnitude of the cross section by a factor of 2 or 3, are the use of an isotropic effective mass for the electrons, an average velocity of sound and a single constant for the interaction of the electron with the transverse and longitudinal acoustic modes, and the characterization of the optical modes by a single energy (Einstein approximation).

3.4 EXPERIMENTAL RESULTS

The results of an experiment on 10 ohm-cm p-type silicon irradiated with 30 MeV electrons are summarized in Table 3. The data τ_ℓ and τ_h represent the measurements of the intercept and slope of a plot of $\tau\,(1 + \frac{\Delta p}{p_o})$ versus $\frac{\Delta p}{p_o}$. The data were reduced in a fashion discussed previously.(4)

It is clear from these data that the high-injection level lifetimes are essentially independent of temperature, but that a strong temperature dependence is observed in the low-injection lifetimes. This observation is gratifying because it represents reasonable agreement with the theory. Noting the relations for p-type silicon,

$$\tau_\ell = \tau_n \left(1 + \frac{p_1}{p_o}\right) + \tau_{po} \left(\frac{n_1}{p_o}\right)$$

and

$$\tau_h = \tau_{no} + \tau_{po} ,$$

Table 3

RESULTS OF 30 MeV ELECTRON IRRADIATION OF 10 OHM-CM p-TYPE SILICON

T (^{o}K)	τ_{ℓ} (μsec)	τ_h (μsec)
278-286	.15 ± .07	7 ± 3
293-298	.3 ± .15	10 ± 5
303-306	.45 ± .15	16 ± 4
312-316	.65 ± .2	16 ± 4
320-326	.95 ± .4	14 ± 5
334-338	1.3 ± .4	8 ± 4
342-345	1.1 ± .4	10 ± 4
350-352	1.9 ± .3	7 ± 4
364-366	2.05 ± .3	9 ± 4
372	2.5 ± .3	7.5 ± 4
374	3.4 ± .3	--
380	4.2 ± 1	--

we can conclude from the lowest temperature measurements that the value of τ_{no} must be less than 0.3 μsec. Hence, from the high-injection lifetime measurements, τ_{po} is $\sim$ 10 μsec. We must therefore assume that the recombination center, if it is a simple one having only two states, has neutral and positive charge states, and that it is therefore a net donor.

At this point there are still two possibilities for the location of the recombination center, either above or below the center of the forbidden energy gap. If we assume it is above the center of the gap, then the temperature dependence of the low-injection lifetime is dominated by the term $\tau_{po}\, n_1/p_o$. We can calculate the consistency of these data since we can assume τ_{po} to be 10 μsec and to have the temperature dependence of a neutral interaction. Alternatively, we can assume that the recombination center lies below the center of the forbidden gap and the dominant term in τ_ℓ will be $\tau_{no} \frac{p_1}{p_o}$. In this case, τ_{no} is assumed to have the temperature dependence of an attractive Coulomb interaction between the electron and the charged donor center.

The experimental data, together with theoretical curves calculated for the two alternative hypotheses, have been plotted in Fig. 4. It can be seen that the curve for the flaw above the center of the gap appears to deviate significantly from the experimental data at high temperatures. On the other hand, the curves representing a net donor below the center of the gap are consistent with the experimental observations. This curve has been fitted to the experimental data at a value of $10^3/T$ of 3.0. This fit results in a value of τ_{no} at this temperature of 0.03 μsec. This value is less than the upper limit placed on τ_{no} by the low temperature value of 0.3 μsec.

Hence, from these data alone, we deduce that the recombination center, which is active in p-type silicon irradiated by high-energy electrons, is a net donor which lies below the center of the forbidden gap and has an activation energy of $\sim$ 0.35 eV. Analysis of more recent experiments with better instrumentation should yield confirmation of these results and produce higher accuracy in the lifetime determinations.

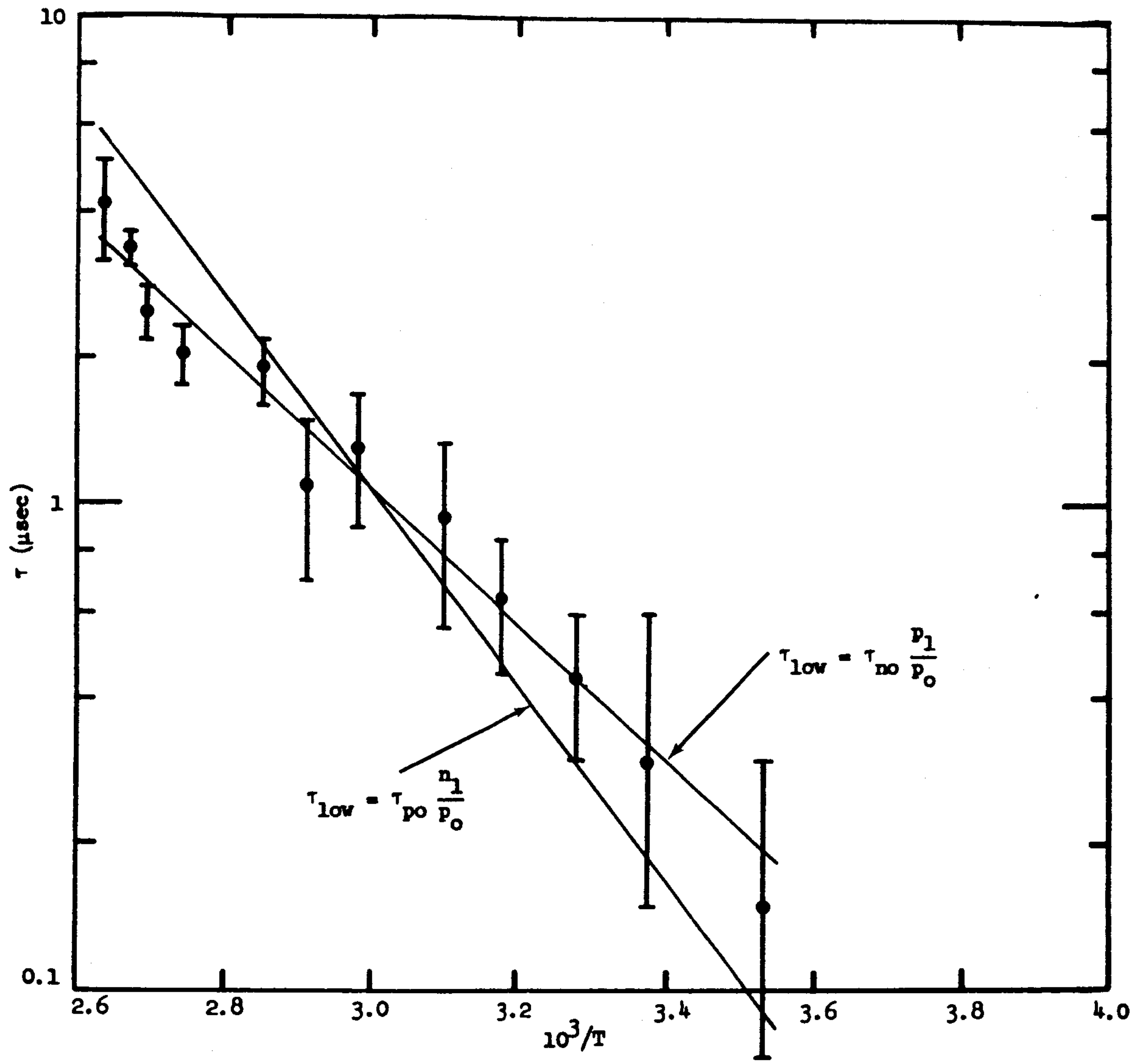

Fig. 4--Measured and theoretical lifetimes, τ_ℓ

3.5 FUTURE PLANS

The immediate task on hand is to analyze the more recent experiments on p-type silicon to determine their consistency with this model and to evaluate the parameters more accurately. Data taken concurrently on n-type silicon will also be analyzed to improve on the information previously generated. These data will then be used to guide electron spin resonance experiments. Studies on material irradiated with 1 to 3 MeV electrons will also be performed.

<u>REFERENCES</u>

1. H. Lintz, S. P. Snowden and V. A. J. van Lint, Radiation Effects on Silicon, Second Quarterly Report Covering the Period September 1 through November 30, 1964, on Contract NAS7-289, General Atomic Report GACD-5974.

2. G. D. Watkins and J. W. Corbett, "Defects in Irradiated Silicon: Electron Paramagnetic Resonance of the Divacancy," Phys. Rev., to be published; J. W. Corbett and G. D. Watkins, "The Production of Divacancies and Vacancies by Electron Irradiation of Silicon," Phys. Rev., to be published.

3. M. Lax, Phys. Rev. 119, 1502 (1960).

4. V. A. J. van Lint, J. W. Harrity, D. K. Nichols and D. P. Snowden, Radiation Effects on Silicon Solar Cells, Technical Summary Report Covering the Period May 16, 1963 through October 15, 1963, on Contract NAS7-91, General Atomic Report GA-4797.